3 Biotech (2020) 10:329
https://doi.org/10.1007/s13205-020-02324-z

ORIGINAL ARTICLE

In vitro growth of *Colletotrichum gloeosporioides* is affected by butyl acetate, a compound produced during the co-culture of *Trichoderma* sp. and *Bacillus subtilis*

Ramírez-Vigil Emanuel[1,3] · Peña-Uribe César Arturo[1] · Macías-Rodríguez Lourdes Iveth[2] · Reyes de la Cruz Homero[1] · Chávez-Avilés Mauricio Nahuam[3]

Received: 18 November 2019 / Accepted: 29 June 2020 / Published online: 3 July 2020

Abstract

The co-culture of plant beneficial microbes to stimulate the production of antimicrobial metabolites is gaining ground. Here, the inactivated *Colletotrichum gloeosporioides* mycelium was used to induce the biosynthesis of antifungal compounds in the co-culture systems of *Trichoderma* sp. and *Bacillus subtilis*. The hexanic extracts obtained from the co-culture systems were tested against *C. gloeosporioides.* Those that inhibited the phytopathogen growth were further fractionated by column and thin-layer chromatography and analyzed by gas chromatography coupled to mass spectrometry (GC–MS). Ethyl butanoate, butyl acetate, acetic acid, 2-butoxyethanol, 3,5-di-tert-butyl-4-hydroxybenzaldehyde, 3,5-di-tert-butyl-4-hydroxybenzyl alcohol, hexadecanoic acid, and octadecanoic acid were identified. Butyl acetate was the most abundant compound, and its application affected the morphology and mycelial development of *C. gloeosporioides*, thereby inhibiting the radial growth, reducing spore formation, and inducing soft colonies. We conclude that co-culturing *Trichoderma* sp. and *B. subtilis* promotes the production of novel diffusible organic compounds with an antifungal effect on *C. gloeosporioides*.

Keywords Anthracnose · Avocado pathogen · Biocontrol · Diffusible organic compounds

Introduction

Avocado (*Persea americana* Mill) is an ancient fruit originally from Central America that has been consumed by local populations, mainly in Mexico, for more than 10,000 years (Araújo et al. 2018; Ayala Silva and Ledesma 2014). Currently, it is one of Mexico's most exported fruits, with Mexico being the most significant contributor to the global market (> 33.6% of the global production) (FAOSTAT 2017). Recent reports have shown that in June 2019, over 1×10^6 tons of avocado were harvested in Mexico, resulting in a net economic gain in the region of $2,000,000,000 (SIAP 2019). Moreover, the avocado demand will increase in the upcoming years. For these reasons, avocado is a significant economic resource in Mexico.

Plant growth and development, including fruit production, are affected by two types of environmental factors: abiotic stress (e.g., soil pH, nutrient and water availability, temperature, and soil salinity) and biotic stress (e.g., pathogenic microorganisms, parasites, weeds, and insects) (Fraire-Velázquez et al. 2011). The latter stress can occur at two different stages in avocado production called as

Electronic supplementary material The online version of this article (https://doi.org/10.1007/s13205-020-02324-z) contains supplementary material, which is available to authorized users.

✉ Reyes de la Cruz Homero
delacruz@umich.mx

✉ Chávez-Avilés Mauricio Nahuam
nchavez@cdhidalgo.tecnm.mx

[1] Laboratorio de Biotecnología Molecular de Plantas, Instituto de Investigaciones Químico Biológicas, Universidad Michoacana de San Nicolás de Hidalgo, Edif. U-3, Ciudad Universitaria, 58030 Morelia, Michoacán, México

[2] Laboratorio de Bioquímica Ecológica, Instituto de Investigaciones Químico Biológicas, Universidad Michoacana de San Nicolás de Hidalgo, Edif. B-3, Ciudad Universitaria, 58030 Morelia, Michoacán, México

[3] Laboratorio de Bioquímica y Biología Molecular, División de Ingeniería Bioquímica, Tecnológico Nacional de México Campus Ciudad Hidalgo, Av. Ing. Carlos Rojas Gutiérrez 2120, Fracc. Valle de la Herradura, 61100 Ciudad Hidalgo, Michoacán, México

pre-harvest and post-harvest stage (Darvas and Kotze 1987). The pre-harvest stress includes diseases such as root rot, caused by the oomycete *Phytophthora cinamonni,* that results in smaller leaves and fruits (Zentmyer 1984). Another example is Cercospora spot, caused by *Cercospora purpurea* (aka *Pseudocercospora purpurea*), that is visible as small brown/purple lesions on leaves and fruits (Pernezny et al. 2000). The post-harvest stress includes diseases that affect the fruit during the ripening process and thus its commercialization. Two significant post-harvest diseases are known to affect avocados: stem-end rot, induced by *Dothiorella* spp., and anthracnose, caused by *Colletotrichum gloeosporioides*. Their general symptoms involve brown spots on the fruit skin and pulp decay (Willingham et al. 2001), thus affecting fruit quality and causing significant economic losses.

Different methods counteract pre- and post-harvest diseases, and the most common one uses chemical fungicides to inhibit pathogen growth (Willingham et al. 2001). However, extensive fungicide use has several drawbacks; for example, it can generate fungicide-resistant pathogens, contaminate the natural environment, and negatively affect the non-pathogenic strains in the ecosystem (Wightwick et al. 2010). Recently, biocontrol agents have emerged as a promising alternative to chemical fungicides. The agents include microorganisms that inhibit pathogen growth, either by competition or by the production of secondary metabolites with antimicrobial effect (Pal and Gardener 2006). Hence, to improve crop yields of commercially important plants, biotechnology research has focused on particular microorganisms that can protect health and prevent diseases (Fira et al. 2018; Gerbore et al. 2014; Kumar and Ashraf 2017). *Trichoderma* and *Bacillus* species, for instance, are well-known natural biocontrol agents due to their capability to produce diverse antifungal compounds such as diffusible and volatile organic compounds (Guzmán-Guzmán et al. 2019; Ashwini and Srividya 2014). *Trichoderma* is a fungus that interacts with other microorganisms in the soil communities, and this interaction stimulates the production of metabolites with antibiotic activity. In this sense, *Bacillus subtilis* strains isolated from the rhizosphere have been used to biocontrol *Macrophomina phaseolina* (Singh et al. 2008) and *Fusarium oxysporum* (Gajbhiye et al. 2010). In addition, *B. subtilis* produces lytic enzymes (chitinases, glucanases, and cellulases) (Živković 2010), and secondary metabolites with biocontrol activity, like antibiotics (Joshi and McSpadden Gardener 2006). Thus, *B. subtilis* is an ideal candidate to use in combination with *Trichoderma* to perform a better biocontrol process. Therefore, this work aimed to evaluate the co-inoculation effect of *Trichoderma* sp. and *B. subtilis* on the biosynthesis of compounds with antifungal activity against *C. gloeosporioides*.

Materials and methods

Strains and propagation

The strains used in this study were *Bacillus subtilis*, *Trichoderma* T1, T2, and T3, and *Colletotrichum gloeosporioides*. All *Trichoderma* strains were grown on potato dextrose agar (PDA) medium (Difco). The isolates were incubated for 10 days (7 days in darkness and 3 days under a 12-h photoperiod to induce sporulation) at 32 ºC. Spores from 10-day-old *Trichoderma* sp. cultures were collected by scraping the surface of the cultures with a spatula and transferred to a 15-mL transparent polypropylene conical-bottom tube with conical bottom and 5 mL of sterile distilled water. The solution was homogenized by agitation for 1 min, filtered through pieces of polypropylene filter cloth (Magitel), and transferred to a clean polypropylene tube. The solution was then serially diluted with sterile distilled water in a 1:10 ratio to perform the spore count using a Neubauer chamber. Spore content values were adjusted and used for subsequent experiments.

C. gloeosporioides was grown from an inoculated propagule from a PDA culture and then incubated at 32 ºC for 10 days. *B. subtilis* was isolated from a commercial solution (Serenade Max, Bayer).

Inactivation of *C. gloeosporioides* mycelium

Four 8-mm diameter plugs of PDA medium covered with *C. gloeosporioides* were grown in 250 mL potato dextrose broth (PDB) medium to initiate mycelial growth. The flasks with PDB medium were incubated at 32 °C for 7 days with constant agitation at 180 rpm. The mycelium was filtered through a membrane and washed three times with sterile distilled water. The collected mycelium was inactivated by boiling in water for 30 min, cooled to room temperature, and then filtered to remove excess water. The mycelium was stored at − 20 °C, until use (Yang, 2009).

Hexanic extract preparation and fractionation by column and thin-layer chromatography (TLC)

1×10^8 colony-forming units of *B. subtilis* were directly co-inoculated with 1×10^7 spores of *Trichoderma* sp. strain (T1, T2, or T3), in 250-mL PDB supplemented with 1% inactivated *C. gloeosporioides* mycelium, and each of the three co-inoculation systems was called as T1, T2, and T3 system, respectively. After a 3-day incubation at room temperature (21 °C) and in the presence of light, the extraction was performed as follows. After filtrating the growth medium, hexane was added in a 1:1 (v/v) ratio to the

co-culture supernatant, and the mix was incubated at room temperature on an orbital shaker at 180 rpm for 3 days. The organic fraction was separated using a funnel and concentrated in a rotary evaporator at 68 °C. The crude extract was separated on a chromatographic column with silica gel serving as the stationary phase and eluted with ethyl acetate–hexane, increasing the polarity by 10% for each fraction (90:10, 80:20, 70:30, 60:40, and 50:50 v/v). The fractions were dried in a rotary evaporator, obtaining a dense yellow oil. Inhibition of *C. gloeosporioides* growth was analyzed by impregnating paper disks (5 mm in diameter) (Kim et al. 1995) with 150 µg/mL of each fraction dissolved in dimethyl sulfoxide (DMSO). The paper disks and a propagule of *C. gloeosporioides* were placed 3 cm apart on PDA medium and incubated at 4 °C for 24 h to allow even spreading, and then at 32 ºC for 9 days.

The fractions with the highest biological activity, determined by highest radial growth inhibition, were separated by thin-layer chromatography (TLC). For this purpose, 100–200 µL of each column fraction were transferred on TLC plates (TLC Silica gel 60 F_{254}) and deposited in chromatographic cells, previously prepared with hexane and ethyl acetate in a 95:5 (v/v) ratio. The plates were observed under UV light (254 nm) and used to determine the retention factor (Rf) for each separated TLC fraction with a ruler. The silica was scraped from the plates, and the fractions with similar Rf values were combined. Each TLC fraction was re-extracted, based on its weight, using hexane, ethyl acetate, or methanol in a 2:1 (v/v) ratio. The effect of each TLC fraction from the supernatants (from the samples vortexed and centrifuged) on *C. gloeosporioides* growth was determined.

Table 1 Fractions obtained by TLC of hexanic extracts from each co-inoculation systems

System	TLC fraction	Chromatographic column fraction	Rf
T1	1	13–38	0.75
	2	1–12	0.62
	3	1–38	0.45
	4	1–12	0.301
	5	1–38	0.307
	6	1–38	0.26
	7	5–7	0.20
	8	1–38	0.15
	9	1–12	0.03
	10	1–9	0.78
T2	1	1–6, 12–24	0.02
	2	6–12, 12–24	0.06
	3	1–60	0.13
	4	5–8	0.18
	5	1–60	0.21
	6	1–72	0.25
	7	4–24	0.29
	8	1–60	0.42
	9	3	0.52
	10	5–6	0.62
	11	1–60	0.75
	12	60–72	0.01
	13	57–65	0.68
	14	61–63	0.70
	15	61–63	0.55
	16	58–65	0.28
	17	49–64	0.036
	18	37–60	0.02
T3	1	1–36	0.08
	2	1–36	0.14
	3	5–7	0.23
	4	5–12	0.29
	5	5–7	0.54
	6	1–72	0.73
	7	1	0.25
	8	26–72	0.18
	9	37–41	0.29
	10	62	0.60

Bioassays of TLC fractions

To assess the antifungal effect of the TLC-extracted fractions 0.5, 1, 1.5, and 2 µL of each was pipetted on 5 mm diameter paper discs and allowed to evenly spread by incubation at 4 °C for 24 h. The TLC fraction-impregnated discs were placed on the PDA medium in a Petri dish. A propagule of *C. gloeosporioides* was put in the center of the Petri dish, approximately 3 cm from each disc. The assay was incubated at 32 ºC for 9 days.

Identification of diffusible compounds

The metabolites in the TLC fractions were identified by GC–MS (Agilent Foster City, CA, USA). The samples were dried using nitrogen gas and re-suspended in 20 µL of ethyl acetate. Then, 1 µL of each sample was injected into the Agilent 6850 Series II gas chromatograph equipped with an Agilent MS detector (model 5973). The ions were detected after electron impact ionization (70 eV). The initial operating conditions were 150 °C for 3 min, followed by a steady increase of 5 °C/min until a final temperature of 278 °C after a total of 12 min. The temperature conditions were as follows: post-run temperature, 300 °C for 3 min; the injection temperature, 270 °C; the detection temperature, 300 °C. The detected compounds were tentatively identified by comparisons from the library (NIST/EPA/NIH Mass Spectral Database 11 and NIST Mass Spectral Search Program 2.0; Chem Station Agilent

Technologies Rev. D.04.00 2002) (Contreras-Cornejo et al. 2009).

Antifungal effect of butyl acetate on *C. gloeosporioides*

PDA medium was supplemented with 0.1, 1, 10, and 100 µM of butyl acetate, to evaluate its effect on the growth of *C. gloeosporioides*. Ethanol-supplemented PDA was used as a control and had the maximum volume of ethanol (200 µL) used to prepare the butyl acetate solutions.

A plug of PDA medium covered with *C. gloeosporioides* (grown on PDA for 10 days) was placed in the center of a Petri dish and grown for 10 days on PDA with a specific concentration of butyl acetate or ethanol. Radial growth inhibition was determined after 10 days using the following equation: growth inhibition = [(Control growth—Treated growth)/(Control growth)] × 100 (Abdelshafy et al. 2020; Arjona-Girona et al. 2014). *C. gloeosporioides* mycelial morphology was analyzed using a light microscope.

Spores collected from the butyl acetate-treated mycelia for 10 days at room temperature in the dark were used to inoculate PDB at a 5×10^4 concentration and evaluate the effect of butyl acetate on *C. gloeosporioides* spore germination. Spore germination and mycelial growth were determined after 1 day or 2 days upon inoculation. Mycelial samples were stained with a drop of brilliant blue and then visualized under a light microscope using the 40 × objective. In addition, a sterile paper disc, placed at the center of the Petri dish with PDA, was inoculated with 2250 spores from the previous treatment and grown for 10 days at 32 ºC. Mycelial morphology was analyzed using a microscope equipped with the Meiji Infinit 1 metallographic camera using the 10 × and 40 × objectives.

Statistical analysis

GraphPad Prism 5 (GraphPad Software Inc, La Jolla, CA) was used to perform statistical analyses. Data were expressed as the means ± SD of three experiments and analyzed by one-way ANOVA followed by the Tukey's post-hoc tests for differences in the percent inhibition of *C. gloeosporioides* growth. Differences were considered significant at $\alpha < 0.01$.

Results

Biocontrol agents produce several secondary metabolites that inhibit the growth of phytopathogens, and their combination have been recommended to improve their efficacy

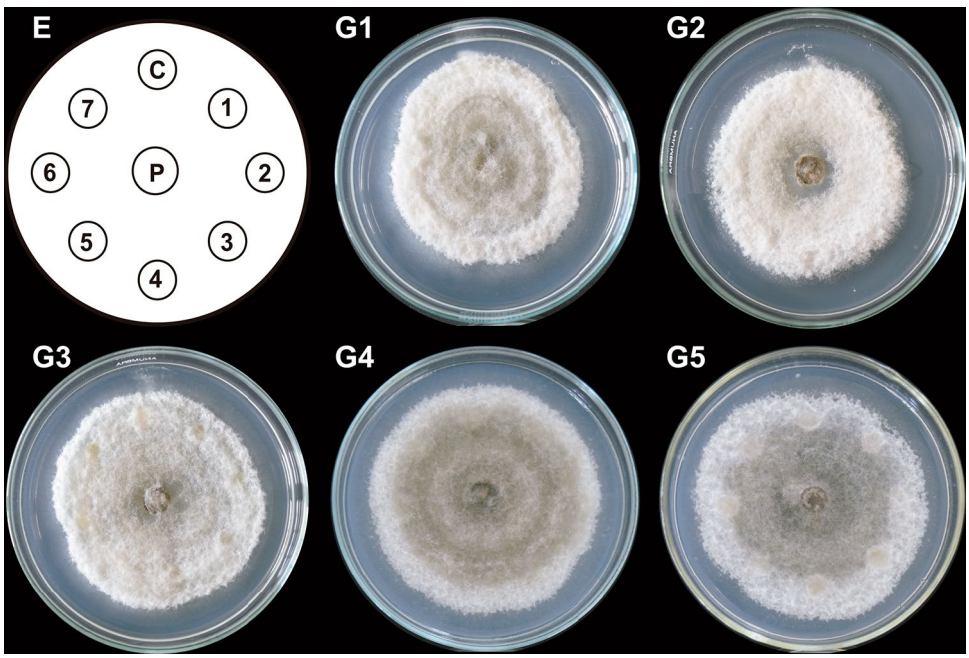

Fig. 1 Antifungal effect of column fractions obtained from T1 system on *C. gloeosporioides* growth. Hexane-extracted compounds synthesized by co-inoculated *B. subtilis*, *Trichoderma* T1 strain, and inactivated *C. gloeosporioides* mycelium (T1 system) were fractionated by column chromatography. Paper discs (1–7 in E) impregnated with 150 µg/mL of each T1 column fraction (1–35) were placed clockwise, 3 cm apart on a PDA-containing Petri dish with a propagule of *C. gloeosporioides* (*P*) in the center. A DMSO-impregnated disc was used as a control (C). The Petri dish was incubated at 4 °C for 24 h and then at 32 ºC for 9 days. Representative images of developed *C. gloeosporioides* mycelia are shown (G1–G5). This experiment was performed in triplicate

(Jambhulkar et al. 2018). Therefore, to induce the biosynthesis of compounds that may inhibit the growth of avocado pathogen *C. gloeosporioides*, this study used a novel system that consisted of co-inoculated biocontrol agents *B. subtilis*, *Trichoderma* sp., and the inactivated *C. gloeosporioides* mycelium. Three tripartite systems were analyzed and named T1, T2, and T3, respectively, based on the strain of *Trichoderma* used. After 3 days, the diffusible organic compounds synthetized by each system were extracted using hexane and fractioned by column chromatography. Each system produced 72 fractions (Supplementary Table 1).

The antifungal capacity of the selected column fractions (≥ 150 µg/mL) from each system (Table 1) on the growth of *C. gloeosporioides* was assessed on the PDA medium containing column fraction impregnated paper discs. Although T1 column fractions could not fully inhibit the radial mycelial growth, they significantly reduced it (Fig. 1, G3 and G5). Moreover, the mycelium developed holes near the discs and in the sporulation areas (Fig. 1, G2, G3 and G5).

On the plates treated with T2 column fractions (Fig. 2; G11), cottony structures formed in the middle of the colonies and sporulation zones. T3 column fractions, furthermore, induced irregular growth and reduced vegetative and

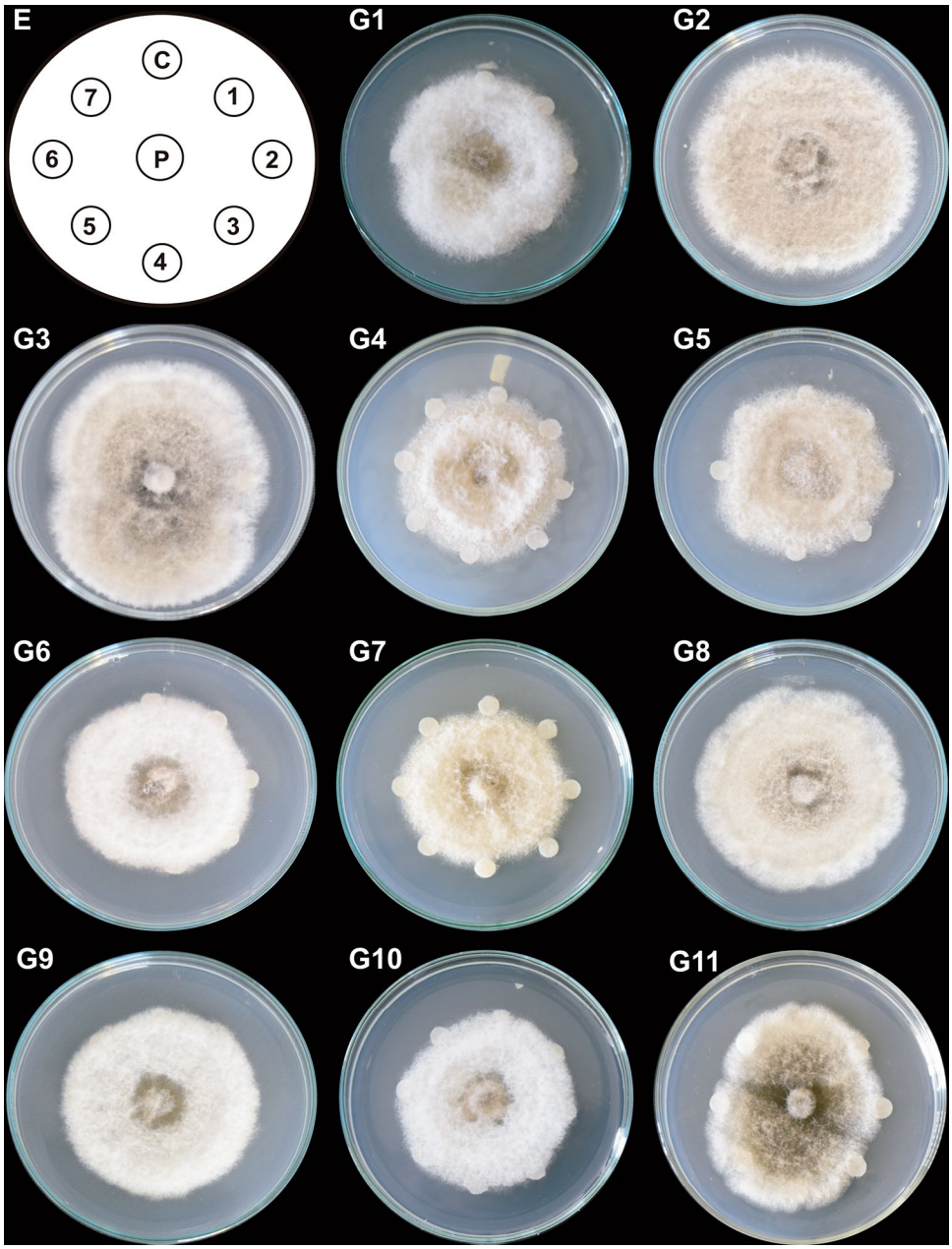

Fig. 2 Antifungal effect of column fractions from T2 system on *C. gloeosporioides* growth. Hexane-extracted compounds synthesized by co-inoculated *B. subtilis*, *Trichoderma* T2 strain, and inactivated *C. gloeosporioides* mycelium (T2 system) were fractionated by column chromatography. Paper discs (1–7 in E) impregnated with 150 µg/mL of each T2 column fraction (1–77) were placed clockwise, 3 cm apart on a PDA-containing Petri dish with a propagule of *C. gloeosporioides* (*P*) in the center. A DMSO-impregnated disc was used as a control (C). The Petri dish was incubated at 4 °C for 24 h and then at 32 ºC for 9 days. Representative images of *C. gloeosporioides* mycelia are shown (G1–G11). Discs impregnated with each column fraction were placed clockwise and numbered consecutively in groups of seven fractions according to the scheme (E). This experiment was performed in triplicate

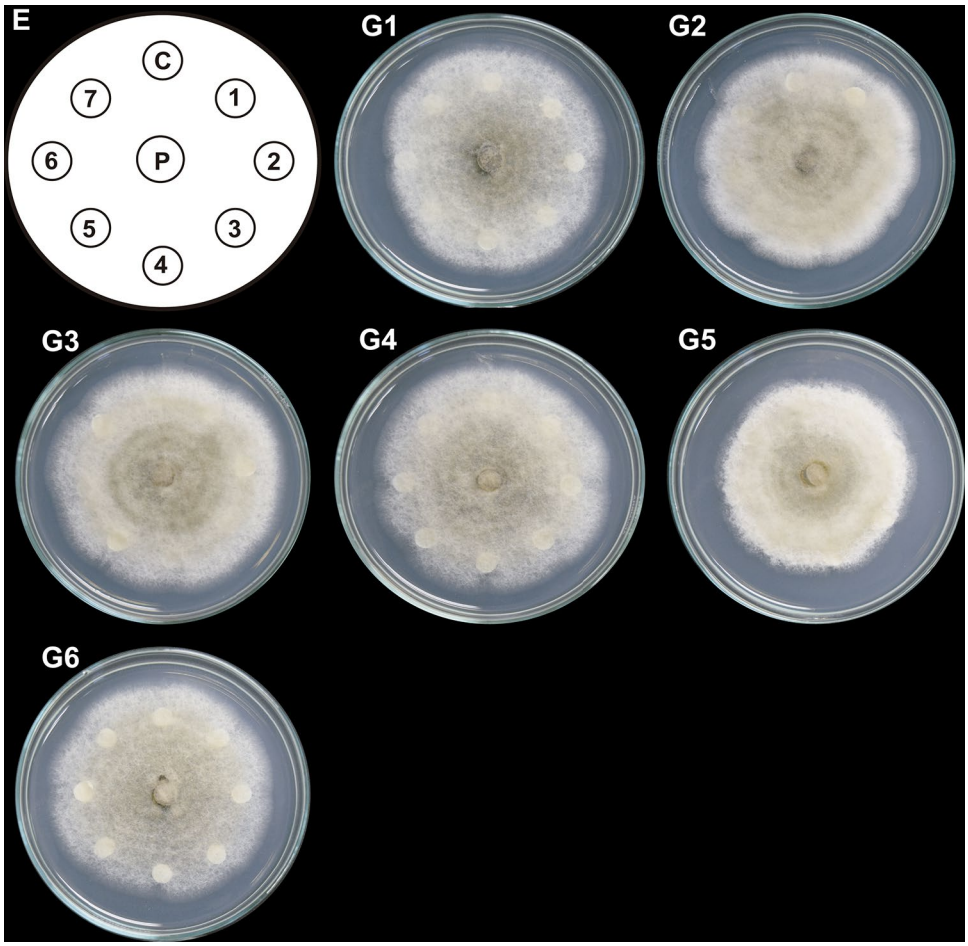

Fig. 3 Antifungal effect of column fractions from T3 system on *C. gloeosporioides* growth. Hexane-extracted compounds synthesized by co-inoculated *B. subtilis*, *Trichoderma* T3 strain, and inactivated *C. gloeosporioides* mycelium (T3 system) were fractionated by column chromatography. Paper discs (1–7 in E) impregnated with 150 µg/mL of each column fraction (1–42) were placed clockwise, 3 cm apart on a PDA-containing Petri dish with a propagule of *C. gloeosporioides* (*P*) in the center. A DMSO-impregnated disc was used as a control (C). The Petri dish was incubated at 4 °C for 24 h and then at 32 °C for 9 days. Representative images of developed *C. gloeosporioides* mycelia are shown (G1–G6). Discs impregnated with each column fraction were placed clockwise and numbered consecutively in groups of seven fractions. This experiment was performed in triplicate

aerial growth (mycelial loosening) around the discs. T3 column fractions (Fig. 3; G5) inhibited the radial mycelial growth. They caused mycelium compaction and sporulation rings that spanned from the central zone to the middle region of the colonies (Fig. 3; fractions in G2, G3, and G4; the first four fractions in G1).

Column fractions with significant effects on the mycelial growth (Table 1) were subjected to TLC to identify the active compounds. The resulting TLC fractions with similar Rf were collected and combined. TLC yielded 18 fractions from T2 and 10 from T1 and T3 (Table 1). Their antifungal effect on the radial growth of *C. gloeosporioides* was assessed on the PDA medium with TLC fraction-impregnated paper discs. Seven T1 TLC fractions inhibited growth that was visible as colony arrest in the areas of contact with the discs (Fig. 4). Cottony structures also formed in the middle of the colonies treated with T1 TLC fractions 7, 8, and 9, while T1 TLC fractions 1 and 6 resulted in mycelial loosening.

In addition, a sporulation zone formed in the center of the colony treated with T1 TLC fractions 4, 5, 7, and 8 and in the entire colony exposed to T1 TLC fractions 1 and 6 (Fig. 4).

Seven out of 18 T2 TLC fractions showed an inhibitory effect on the radial mycelial growth (Fig. 5). Growth arrest was also present when the mycelium reached the edge of the discs impregnated with T2 TLC fractions 10, 11, and 18 (Fig. 5). These effects were thus different from those triggered by T1 TLC fractions, where mycelial loosening on discs treated with T2 TLC fractions 3, 4, 6, and 14 (Fig. 5) developed. In the T2 TLC fraction 3, mycelial growth-arrested and lack of sporulation rings were also observed (Fig. 5).

Finally, 7 out of 10 T3 TLC fractions (Fig. 6) affected *C. gloeosporioides* growth. When the mycelium reached the edges of discs impregnated with T3 TLC fractions 1, 2, and 3, loosening occurred. This effect was most prominent in T3 TLC fractions 4, 6, 8, and 10. Moreover, the radial growth ceased, and the flattening of colonies enhanced with increasing volumes of added T3 TLC fractions, except in T3 TLC fraction 8, where this effect appeared at all fraction volumes. In the latter, the colonies were also both loose or compact (Fig. 6).

The TLC fractions with higher inhibitory activities were selected for GC–MS analysis. Eight compounds were identified: ethyl butanoate, butyl acetate, acetic acid,

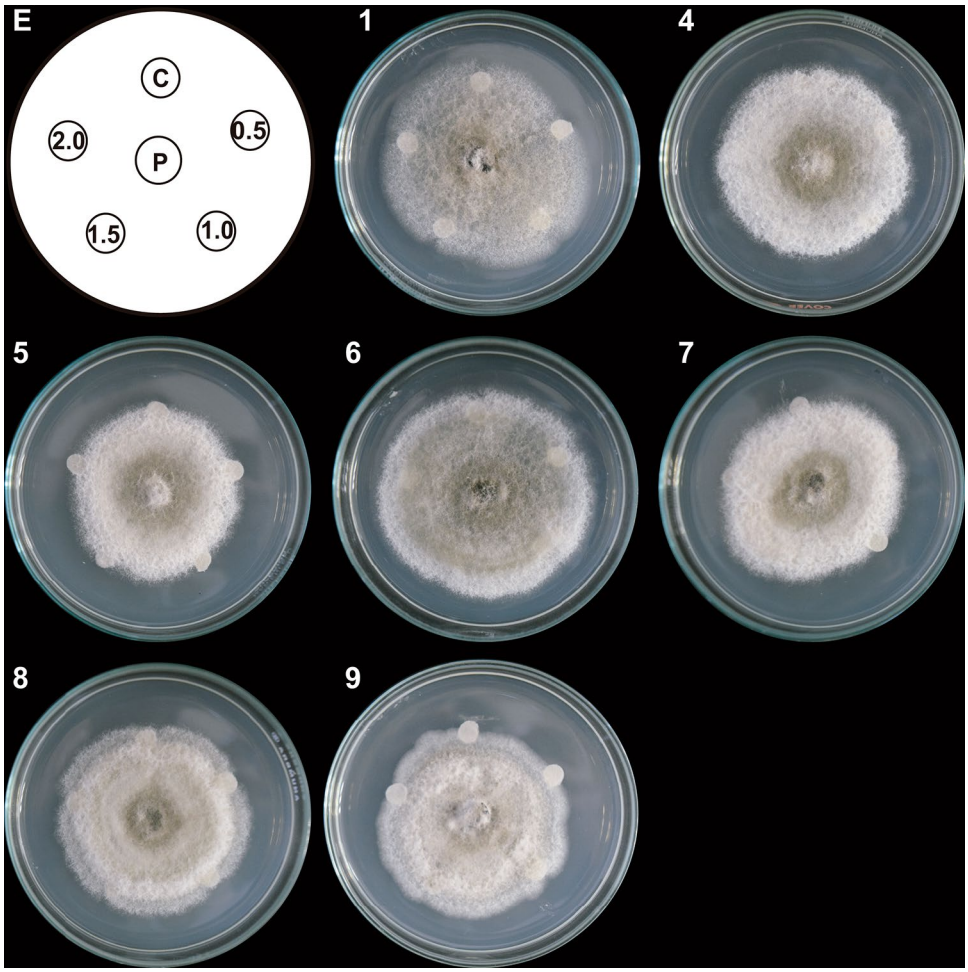

Fig. 4 Antifungal effect of TLC fractions obtained from the T1 system on *C. gloeosporioides* growth. Hexane-extracted compounds synthesized by co-inoculated *B. subtilis*, *Trichoderma* T1 strain, and inactivated *C. gloeosporioides* mycelium (T1 system) were fractionated with TLC. Paper discs impregnated with 0.5, 1.0, 1.5, and 2.0 µL of the TLC fractions were placed clockwise on a Petri dish (E). A propagule of *C. gloeosporioides* (*P*) was placed in the center, 3 cm away from the discs. A DMSO-impregnated disc was used as a control (C). The Petri dish was incubated at 4 °C for 24 h and then at 32 °C for 9 days. Representative images of developed *C. gloeosporioides* mycelia (1, 4, 5, 6, 7, 8, and 9). Only those images of TLC fractions with a demonstrated effect on pathogen growth are shown. This experiment was performed in triplicate

2-butoxyethanol, 3,5-di-tert-butyl-4-hydroxybenzaldehyde, 3,5-di-tert-butyl-4-hydroxybenzyl alcohol, Hexadecanoic acid, and Octadecanoic acid (Table 2). As butyl acetate was the most abundant compound in all active fractions (Table 3), its effect on *C. gloeosporioides* was tested. Radial mycelial growth and morphology were evaluated on PDA media supplemented with increasing concentrations of butyl acetate (0.1, 1, 10, and 100 µM, respectively). The lowest concentration of butyl acetate (0.1 µM) inhibited the radial growth by 9.98% as compared to that in the control (Fig. 7a–d). Conversely, higher levels did not affect growth (Fig. 7a).

Butyl acetate also caused morphological changes at every analyzed concentration; therefore, microscopic analysis was performed to assess the cellular effects. The analysis revealed that butyl acetate caused a dose-dependent hyphal thinning and formation of septate hyphae at 10 µM (Fig. 7b).

Subsequent quantitation of *C. gloeosporioides* spores showed butyl acetate could not affect sporulation (Fig. 7c).

The effect of butyl acetate on spore germination was also evaluated. Spores recovered from *C. gloeosporioides* colonies exposed to 0.1, 1, 10, and 100 µM of butyl acetate were inoculated in PDB or PDA medium (Fig. 8). Microscopic analysis revealed cell wall thinning on the hyphae developed from PDB-germinated spores. This effect was dose-dependent, with the thinning most evident at higher levels of the compound (Fig. 8a). Furthermore, after 2 days of spore incubation, septate hyphae appeared on the germinated spores recovered from colonies grown in 10 µM and 100 µM of butyl acetate, respectively (Fig. 8a, arrowheads).

Spores recovered from colonies treated with the highest concentration (100 µM) of butyl acetate on PDA medium (this concentration showed to be the most significant effector on hyphae morphology in PDB) were further analyzed because this concentration of the compound showed the highest effect on the morphology. In this experiment (Fig. 8b), spores recovered from colonies grown on ethanol-supplemented PDA were used as a control. The results showed that the mycelium developed from spores recovered from colonies grown on both ethanol and PDA for 10 days, and generated a sporulation zone in the center. However, this effect was absent in the mycelium developed from spores recovered from control colonies (Fig. 8b). Remarkably, the mycelium developed from spores recovered from butyl

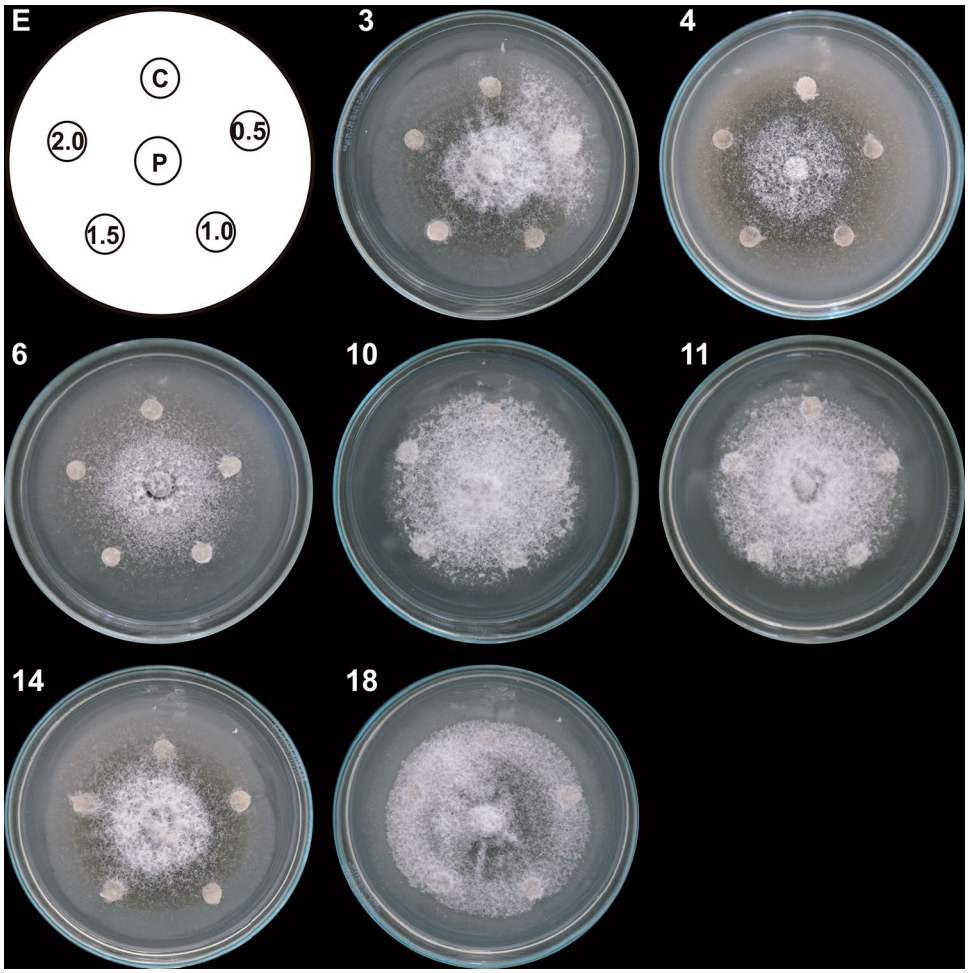

Fig. 5 Antifungal effect of TLC fractions obtained T2 system on *C. gloeosporioides* growth. Hexane-extracted compounds synthesized by co-inoculated *B. subtilis*, *Trichoderma* T2 strain, and inactivated *C. gloeosporioides* mycelium (T2 system) were fractionated with TLC. Paper discs impregnated with 0.5, 1.0, 1.5, and 2.0 µL of the TLC fractions were placed clockwise on a Petri dish (E). A propagule of *C. gloeosporioides* (*P*) was placed in the center, 3 cm away from the discs. A DMSO-impregnated disc was used as a control (C). The Petri dish was incubated at 4 °C for 24 h and then at 32 °C for 9 days. Representative images of developed *C. gloeosporioides* mycelia (3, 4, 6, 10, 11, 14, and 18). Only those images of TLC fractions with a demonstrated effect on pathogen growth are shown (3, 4, 6, 10, 11, 14, and 18). This experiment was performed in triplicate

acetate-grown colonies had loose morphology at its edges and malformations visible as holes in the center and middle zones (Fig. 8b).

Slight sporulation was also noticeable as compared to the mycelium developed under control conditions. Microscopic analysis (Fig. 8c) revealed that the mycelium developed from spores recovered from both control and ethanol treatments did not show morphological differences; in both treatments, hyphae with thick cell walls were observed. Nonetheless, the mycelium developed from spores recovered from butyl acetate-treated colonies displayed septate and lax hyphae (Fig. 8c, arrowhead). Besides, these colonies had fewer hyphae suggesting that these colonies are more susceptible to mechanical damage caused by the sampling procedure.

Discussion

Mexico is the leading global producer and exporter of avocado (*Persea americana* Mill) (FAOSTAT 2017). However, various biotic factors, such as diseases that directly affect the fruit, can cause production losses and exert an impact on international trade (Trinidad-Ángel et al. 2017). Among these diseases, anthracnose caused by *Colletotrichum* spp. is one of the most critical illnesses provoked on the 'Hass' avocado. The infection reduces the fruit quality, not only as a result of direct damage by rots generated directly on the fruit but also because it limits commercialization (Rojo-Báez et al. 2017). The control of fungal diseases mainly depends on chemical fungicides, but because of their toxicity and generation of pathogen resistance, alternatives for treatment are necessary.

Biocontrol agents have emerged as a promising alternative to classical fungicides (Sharma et al. 2009). An exciting candidate among them is *B. subtilis*, due to a large number of antimicrobial metabolites (e.g., non-ribosomally cyclic peptides and volatile organic compounds) that it produces (Mohammadipour et al. 2009). Likewise, *Trichoderma* spp. have been used for biological control due to their ability to colonize different substrates and survive in a wide plethora of habitats (Sharma et al. 2017).

Here, a tripartite system consisting of co-cultured of *Trichoderma* sp., *B. subtilis* and inactivated *C. gloeosporioides* mycelium was used to identify novel compounds that

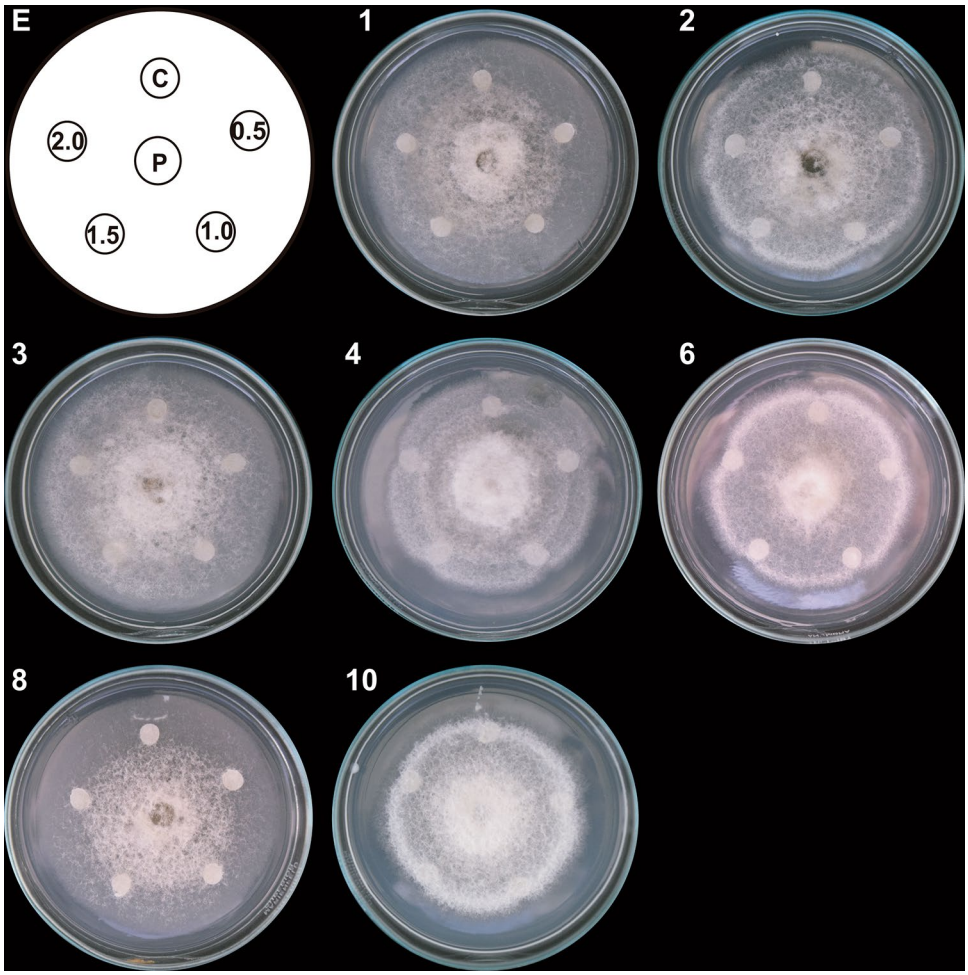

Fig. 6 Antifungal effect of TLC fractions from T3 system on *C. gloeosporioides* growth. Hexane-extracted compounds synthesized by co-inoculated *B. subtilis*, *Trichoderma* T3 strain, and inactivated *C. gloeosporioides* mycelium (T3 system) were fractionated with TLC. Paper discs impregnated with 0.5, 1.0, 1.5, and 2.0 µL of the TLC fractions were placed clockwise on a Petri dish (E). A propagule of *C. gloeosporioides* (P) was placed in the center, 3 cm away from the discs. The Petri dish was incubated at 4 °C for 24 h and then at 32 °C for 9 days. A DMSO-impregnated disc was used as a control (C). Representative images of developed *C. gloeosporioides* mycelia (1, 2, 3, 6, 8, and 10). Only those images of TLC fractions with a demonstrated effect on pathogen growth are shown (1, 2, 3, 6, 8, and 10). This experiment was performed in triplicate

Table 2 Compounds from TLC fractions identified using GC–MS

Compound	Retention time (min)
Ethyl butanoate	5.02
Butyl acetate	5.43
Acetic acid	5.69
2-Butoxyethanol	8.15
3,5-Di-tert-butyl-4-hydroxybenzaldehyde	31.28
3,5-Di-tert-butyl-4-hydroxybenzyl alcohol	31.395
Hexadecanoic acid	35.21
Octadecanoic acid	38.93

Compounds were tentatively identified using the NIST library

could treat anthracnose. Extracts from co-culture supernatants were separated into fractions by column chromatography (Table 1, Supplementary Table 1), and their antifungal effects were evaluated. Although column fractions obtained from T1 and T3 systems did not inhibit *C. gloeosporioides* growth (Figs. 1 and 3), several fractions from T2 system did (Fig. 2).

In addition, all assessed column fractions showed changes in the pathogen growth, such as decreased mycelium density, mycelial damage (i.e., holes), the formation of cottony structures, presence of sporulation zones, and mycelium compaction (Figs. 1–3). These observations indicate that the metabolites present in column fractions indeed have antifungal properties against *C. gloeosporioides*. Column fractions that had the highest growth inhibitory effect on *C. gloeosporioides* were analyzed by TLC. Some resulting TLC fractions altered the growth of *C. gloeosporioides* (Figs. 4–6), and the induced changes were similar to those mentioned above (e.g., growth arrest, mycelial loosening, cottony structures, etc.).

TLC fractions promoted effects similar to those caused by mutations of known genes. For instance, deletions of *CgCdc42* (Wang et al. 2018), *CgRGS1* (Liu et al. 2018), or *CgMK1* (He et al. 2017) resulted in mycelial vegetative and aerial growth inhibition, conidiation, and biomass accumulation. Therefore, we speculate that compounds produced by the co-culture systems affect signaling pathways that regulate growth and development. Alternatively, the compounds may control different pathways and underscore the necessity for future investigation.

Table 3 Metabolites from TLC fractions identified using GC–MS for each of the co-inoculation systems

System-Fraction	Ethyl butanoate	Butyl acetate	Acetic acid	2-Butoxyethanol	3,5-Di-*tert*-butyl-4-hydroxybenzaldehyde	3,5-Di-*tert*-butyl-4-hydroxybenzyl alcohol	Hexadecanoic acid	Octadecanoic acid
	Normalized amount (%)							
T1-1	2.7	8.5	10.2	78.6	nd	nd	nd	nd
T1-4	28.9	71.1	nd	nd	nd	nd	nd	nd
T1-5	nd	71.0	nd	29.0	nd	nd	nd	nd
T1-6	Trace	100.0	nd	nd	nd	nd	nd	nd
T1-7	nd	100.0	nd	nd	nd	Trace	nd	nd
T1-8	14.0	40.8	32.9	nd	Trace	12.3	nd	nd
T1-9	25.3	74.7	nd	nd	nd	nd	nd	nd
T2-3	19.5	59.6	nd	nd	nd	20.9	nd	nd
T2-4	18.9	69.7	nd	nd	Trace	11.4	nd	nd
T2-6	10.9	47.3	nd	nd	18.5	23.3	nd	nd
T2-10	15.6	48.8	nd	nd	8.5	27.1	nd	nd
T2-11	12.7	31.9	nd	nd	55.4	Trace	nd	nd
T2-14	38.3	61.7	nd	nd	nd	nd	nd	nd
T2-18	16.4	51.4	32.2	nd	nd	nd	nd	nd
T3-1	13.2	57.8	nd	nd	nd	29.0	nd	nd
T3-2	26.0	74.0	nd	nd	Trace	Trace	nd	nd
T3-3	12.3	41.4	21.1	nd	Trace	25.2	nd	nd
T3-4	27.0	73.0	nd	nd	nd	Trace	nd	nd
T3-6	9.4	33.8	nd	nd	56.8	Trace	nd	nd
T3-8	2.8	9.2	nd	nd	8.6	5.2	23.2	51.0
T3-10	15.6	54.9	nd	nd	7.6	21.9	nd	nd

nd Not determined

TLC fractions with the highest bioactivity were analyzed by GC–MS to identify the compounds. Among them, butyl acetate was detected in 17 of the 21 analyzed TLC fractions, making up between 8.5% and 100% of each, and is the most abundant of the isolated diffusible compounds (Table 3). Butyl acetate is one of the main volatile organic compounds (VOCs) produced by *Ceratocystis fimbriata* in the biocontrol of *Monilinia fructicola* and *Penicillium digitatum* (Li et al. 2015). Ethyl butanoate was the second most abundant identified compound, detected in 18 fractions, and comprising between 2.7% and 38.3% of each (Table 3). It is a VOC produced by *Saccharomyces cerevisiae* in the biocontrol of *P. digitatum* (de Souza et al. 2018).

2-Butoxyethanol was present in only two fractions, constituting between 29% and 78.6% of each (Table 3). Yuan et al. (2017) reported that this compound is among the VOCs produced by *Bacillus amyloliquefaciens* NJN-6 (Yuan et al. 2017). Furthermore, in 9 fractions, 3,5-di-*tert*-butyl-4-hydroxybenzyl alcohol was identified, ranging between 5.2% and 29% in each (Table 3). This compound has been used as a precursor of hydrocarbon antioxidants (Singh et al. 2017), suggesting that it likely prevents oxidation of hydrocarbon compounds generated during the co-culture (Brown et al. 2008; Hirpara et al. 2016).

In 6 fractions, 3,5-di-*tert*-butyl-4-hydroxybenzaldehyde was detected in amounts ranging between 7.6% and 56.8% (Table 3). Siddiquee et al. (2012) reported this compound as one of the VOCs produced by *Trichoderma harzianum* that is used to control vectors of human diseases: *Culex quinquefasciatus* Say and *Aedes aegypti* Linn (Chellappandian et al. 2018; Siddiquee et al. 2012).

Other identified compounds were as follows: acetic acid, found in 4 fractions and ranging between 10.2% and 32.9% of each; octadecanoic acid, identified in T3-8 fraction and representing 51% of the active compound; and hexadecanoic acid, also present in T3-8 fraction and constituting 23.2% (Table 3). These compounds acidify the growth medium and prevent *C. gloeosporioides* pathogenicity (Guetsky et al. 2005; Kumar et al. 2018).

Since butyl acetate was the most abundant compound, its effect on the growth of *C. gloeosporioides* was analyzed. At the lowest concentrations (0.1 µM), butyl acetate induced the radial growth inhibition by 9.98% when compared to that in the control (Fig. 7). Moreover, microscopic analyses revealed that it reduced spore formation and promoted

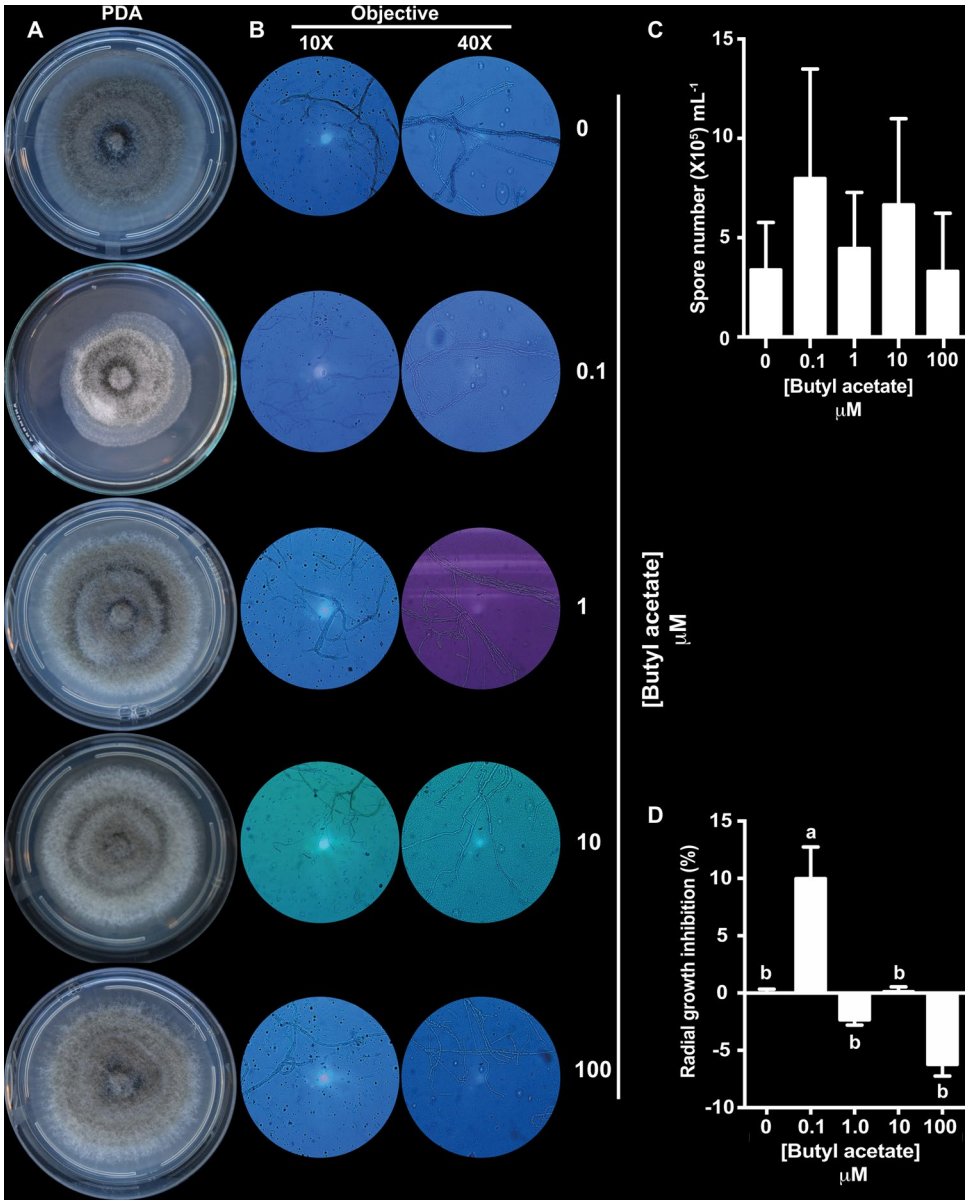

Fig. 7 Effect of butyl acetate on *C. gloeosporioides* growth, mycelial morphology, and spore number. **a** Representative images of *C. gloeosporioides* mycelial growth under control conditions and on indicated concentrations of butyl acetate after a 10-day incubation at room temperature in the dark. **b** Representative micrographs of mycelium from **a**. Mycelial samples were mixed with a drop of brilliant blue and visualized under a microscope with 10 × and 40 × objectives. **c** Quantification of *C. gloeosporioides* spores after treatment with butyl acetate. Bars represent the median spore number ± SE ($n = 3$). **d** Percentage of *C. gloeosporioides* radial growth inhibition (data represent the median ± SE; $n = 4$). Different letters represent statistically different means ($\alpha < 0.01$ in the Tukey's post-hoc test). Three biological experiments were performed

hyphal cell wall thinning that worsened with increasing concentrations. Liu et al. (2011) showed that cinnamaldehyde led to abnormal mycelial morphology, conidial cell wall degradation, and abolished the production of spores on *C. gloeosporioides*. In addition, it induced septated (divided) hyphae at 10 and 100 µM. Thus, the dose-dependent phenotype triggered by butyl acetate might be a result of the loss of cell-wall integrity caused by the impairment of cell wall homeostasis (Bae et al. 2016).

Butyl acetate may also affect the activity of *C. gloeosporioides* laccases that are responsible for melanin biosynthesis and pathogenicity. The *Dlac1* mutant has less pigmentation, drastically reduced aerial mycelial mass, and lower radial growth rates when compared to the wild-type strain (Wei et al. 2017). Indeed, spores that germinated from the butyl acetate-treated *C. gloeosporioides* mycelium produced thinner and septated hyphae, and this effect was more pronounced with higher concentrations of butyl acetate.

Likewise, colonies from the PDA-germinated spores did not have the same dark pigmentation as the control (Fig. 8). Thinner and septated hyphae also developed, indicating that butyl acetate compromised the pathogenicity of *C. gloeosporioides* by constraining hyphal growth.

The fungal membrane has a fundamental role in maintaining cellular homeostasis (Avis, 2007). Antifungal compounds that disrupt the membrane increase its fluidity; these elevations in fluidity will cause generalized disorganization. Since butyl acetate induced hyphal thinning, cell wall degradation, and cell lysis, it could affect both membrane and cell wall integrity.

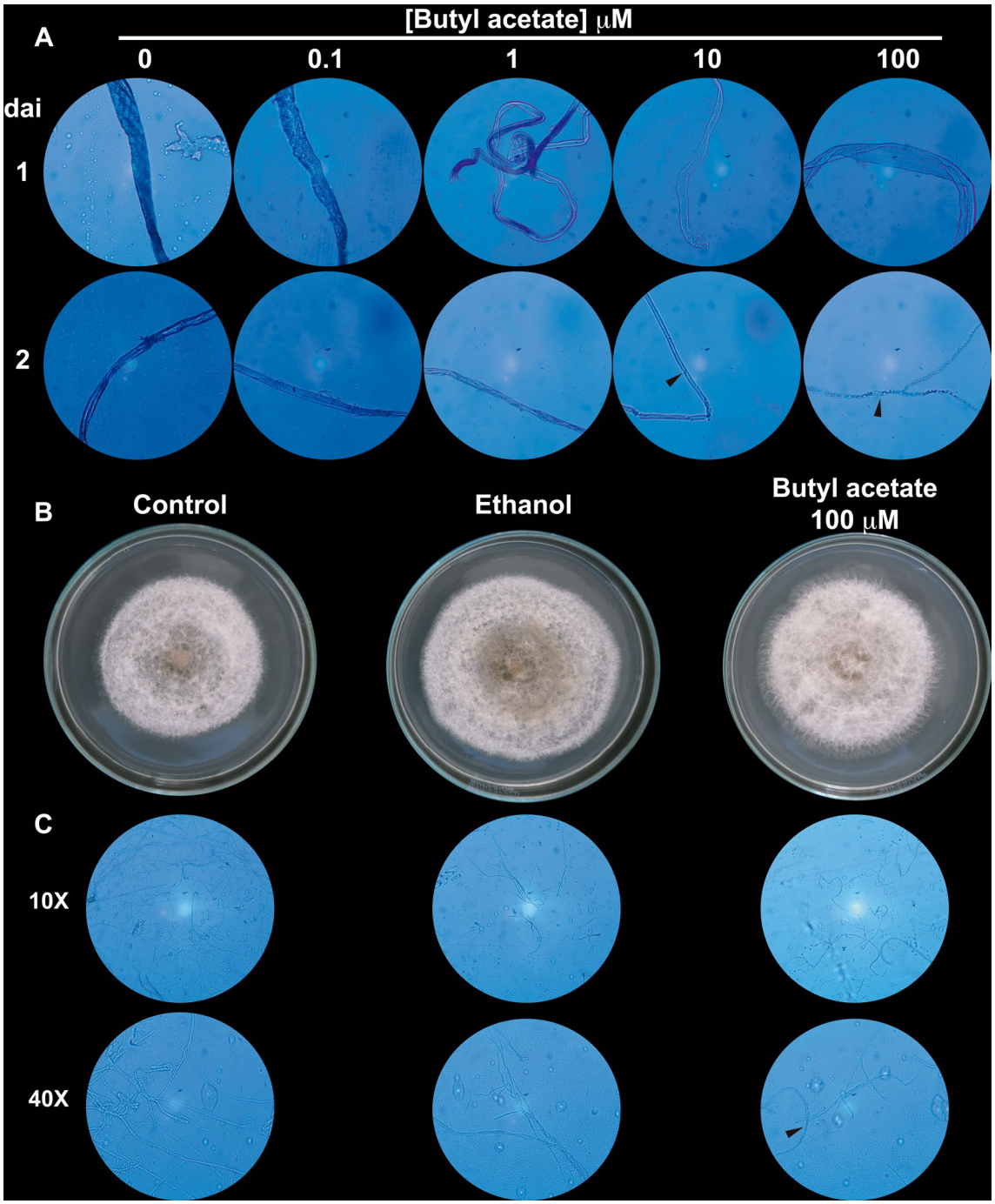

Fig. 8 Effect of butyl acetate on germination of *C. gloeosporioides* spores. **a** Representative micrographs of mycelium from spores germinated in PDB medium. Spores prepared from *C. gloeosporioides* were grown in PDB supplemented with ethanol (0) and indicated concentrations of butyl acetate for 10 days at room temperature in the dark. Mycelial samples were stained with a drop of brilliant blue and then visualized under a microscope using the 40 × objective. Samples were taken 1 day or 2 days after inoculation (dai). **b** Representative images of *C. gloeosporioides* grown in PDB alone for 10 days. Spores were prepared from *C. gloeosporioides* grown on PDA (control), PDA supplemented with ethanol, or PDA supplemented with 100 μM of butyl acetate for 10 days at room temperature in the dark. **c** Representative micrographs of the mycelium from **b**. Mycelial samples were stained with a drop of brilliant blue and visualized under a microscope with 10 × and 40 × objectives

Butyl acetate substantially inhibited growth of *C. gloeosporioides*. It induced drastic changes in spore germination and mycelium development, suggesting a reduction in pathogenicity. However, in vivo analysis is necessary to confirm this assumption. Likewise, whether butyl acetate can manage anthracnose in combination with other compounds is an open question for future research. In summary, our results indicate that the co-culture of *Trichoderma* sp. and *B. subtilis* is a suitable strategy to identify antifungal compounds for the biocontrol of *C. gloeosporioides*.

Acknowledgements The strains used were kindly donated: *Trichoderma* T1 and T3 by Juan Boyzo Marín, *Trichoderma* T2 by M.C. Alberto Flores García from Instituto de Investigaciones Químico Biológicas (IIQB-UMSNH), and the phytopathogenic fungus *C. gloeosporioides* by Dra. Silvia Patricia Hernández Pavia from Instituto de Investigaciones Agropecuarias y Forestales (IIAF-UMSNH). Manuscript editing was supported by Conacyt, grant No. 222405.

Author contributions R-VE conducted the experiments and analyzed the results, P-UCA contributed to study design and edited the manuscript, M-RLI conducted the GC–MS analyses, RCH edited, reviewed and approved the version to be published. C-AMN contributed to overall study design and discussion and edited the manuscript; all authors read and reviewed the manuscript.

Compliance with ethical standards

Conflict of interest The authors declare that they have no conflict of interest.

Ethical statement This article does not contain any studies with human participants or animals performed by any of the authors.

References

Abdelshafy Mohamad OA, Ma JB, Liu YH, Zhang D, Hua S, Bhute S et al (2020) Beneficial endophytic bacterial populations associated with medicinal plant *Thymus vulgaris* alleviate salt stress and confer resistance to *Fusarium oxysporum*. Front Plant Sci 11:47. https://doi.org/10.3389/fpls.2020.00047

Araújo RG, Rodriguez-Jasso RM, Ruiz HA, Pintado MME, Aguilar CN (2018) Avocado by-products: nutritional and functional properties. Trends Food Sci Technol. https://doi.org/10.1016/j.tifs.2018.07.027

Arjona-Girona I, Vinale F, Ruano-Rosa D, Lorito M, López-Herrera CJ (2014) Effect of metabolites from different *Trichoderma* strains on the growth of *Rosellinia necatrix*, the causal agent of avocado white root rot. Eur J Plant Pathol 140(2):385–397. https://doi.org/10.1007/s10658-014-0472-z

Ashwini N, Srividya S (2014) Potentiality of *Bacillus subtilis* as biocontrol agent for management of anthracnose disease in chilli caused by *Colletotrichum gloeosporioides* OGC1. 3Biotech 4(2):127–136. https://doi.org/10.1007/s13205-013-0134-4

Avis TJ (2007) Antifungal compounds that target fungal membranes: applications in plant disease control. Can J Plant Path 29(4):323–329. https://doi.org/10.1080/07060660709507478

Ayala Silva T, Ledesma N (2014) Avocado history, biodiversity and production. In: Nandwani D (ed) Sustainable horticultural systems. Sustainable development and biodiversity, vol 2. Springer, Cham, pp 157–205. https://doi.org/10.1007/978-3-319-06904-3_8

Bae SJ, Mohanta TK, Chung JY, Ryu M, Park G, Shim S et al (2016) *Trichoderma* metabolites as biological control agents against *Phytophthora* pathogens. Biol Control 92:128–138. https://doi.org/10.1016/j.biocontrol.2015.10.005

Brown SH, Yarden O, Gollop N, Chen S, Zveibil A, Belausov E, Freeman S (2008) Differential protein expression in *Colletotrichum acutatum*: Changes associated with reactive oxygen species and nitrogen starvation implicated in pathogenicity on strawberry. Mol Plant Pathol 9:171–190. https://doi.org/10.1111/j.1364-3703.2007.00454.x

Chellappandian M, Thanigaivel A, Vasantha-Srinivasan P, Edwin ES, Ponsankar A, Selin-Rani S, Kalaivani K, Senthil-Nathan S, Benelli G (2018) Toxicological effects of *Sphaeranthus indicus* Linn. (Asteraceae) leaf essential oil against human disease vectors, *Culex quinquefasciatus* Say and *Aedes aegypti* Linn., and impacts on a beneficial mosquito predator. Environ Sci Pollut Res 25:10294–10306. https://doi.org/10.1007/s11356-017-8952-2

Contreras-Cornejo HA, Macías-Rodríguez L, Cortés-Penagos C, López-Bucio J (2009) *Trichoderma virens*, a plant benefical fungus, enhances biomass production and promotes lateral root growth through an auxin-dependent mechanism in *Arabidopsis*. Plant Physiol 149(3):1579–1592. https://doi.org/10.1104/pp.108.130369

Darvas J, Kotze J (1987) Fungi associated with pre-and postharvest diseases of avocado fruit at Westfalia Estate, South Africa. Phytophylactica 19:83–85

de Souza JRB, Kupper KC, Augusto F (2018) *In vivo* investigation of the volatile metabolome of antiphytopathogenic yeast strains active against *Penicillium digitatum* using comprehensive two-dimensional gas chromatography and multivariate data analysis. Microchem J 141:362–368. https://doi.org/10.1016/j.microc.2018.05.047

FAOSTAT (2017) Agricultural avocado statistics: area harvested, yield and production quantity. http://www.fao.org/faostat/en/#data/QC. Accessed 1 Sept 2019

Fira D, Dimkić I, Berić T, Lozo J, Stanković S (2018) Biological control of plant pathogens by *Bacillus* species. J Biotechnol 285:44–55. https://doi.org/10.1016/j.jbiotec.2018.07.044

Fraire-Velázquez S, Rodríguez-Guerra R, Sánchez-Calderón L (2011) Abiotic and biotic stress response crosstalk in plants. In: Shanker A (ed) Abiotic stress response in plants - physiological, biochemical and genetic perspectives. Intech Open. https://doi.org/10.5772/23217

Gajbhiye A, Rai AR, Meshram SU, Dongre AB (2010) Isolation, evaluation and characterization of *Bacillus subtilis* from cotton rhizospheric soil with biocontrol activity against *Fusarium oxysporum*. World J Microbiol Biotechnol 26(7):1187–1194. https://doi.org/10.1007/s11274-009-0287-9

Gerbore J, Benhamou N, Vallance J, Le Floch G, Grizard D, Regnault-Roger C, Rey P (2014) Biological control of plant pathogens: advantages and limitations seen through the case study of *Pythium oligandrum*. Environ Sci Pollut Res 21:4847–4860. https://doi.org/10.1007/s11356-013-1807-6

Guetsky R, Kobiler I, Wang X, Perlman N, Gollop N, Avila-Quezada G, Hadar I, Prusky D (2005) Metabolism of the flavonoid epicatechin by laccase of *Colletotrichum gloeosporioides* and its effect on pathogenicity on avocado fruits. Phytopathology 95:1341–1348. https://doi.org/10.1094/PHYTO-95-1341

Guzmán-Guzmán P, Porras-Troncoso MD, Olmedo-Monfil V, Herrera-Estrella A (2019) *Trichoderma* species: Versatile plant symbionts. Phytopathology 109(1):6–16. https://doi.org/10.1094/PHYTO-07-18-0218-RVW

He P, Wang Y, Wang X, Zhang X, Tian C (2017) The mitogen-activated protein kinase CgMK1 governs appressorium formation, melanin synthesis, and plant infection of *Colletotrichum gloeosporioides*. Front Microbiol 8:2216. https://doi.org/10.3389/fmicb.2017.02216

Hirpara DG, Gajera HP, Bhimani RD, Golakiya BA (2016) The SRAP based molecular diversity related to antifungal and antioxidant bioactive constituents for biocontrol potentials of *Trichoderma* against *Sclerotium rolfsii* Scc. Curr Genet 62:619–641. https://doi.org/10.1007/s00294-016-0567-5

Jambhulkar PP, Sharma P, Manokaran R, Lakshman DK, Rokadia P, Jambhulkar N (2018) Assessing synergism of combined applications of *Trichoderma harzianum* and *Pseudomonas fluorescens* to control blast and bacterial leaf blight of rice. Eur J Plant Pathol 152(3):747–757. https://doi.org/10.1007/s10658-018-1519-3

Joshi R, McSpadden Gardener BB (2006) Identification and characterization of novel genetic markers associated with biological control activities in *Bacillus subtilis*. Phytopathology 96(2):145–154. https://doi.org/10.1094/PHYTO-96-0145

Kim J, Marshall MR, Wei CI (1995) Antibacterial activity of some essential oil components against five foodborne pathogens. J Agricult Food Chem 43(11):2839–2845

Kumar M, Ashraf S (2017) Role of trichoderma spp. as a biocontrol agent of fungal plant pathogens. In: Kumar V, Kumar M, Sharma S, Prasad R (eds) Probiotics and plant health. Springer, Singapore, pp 497–506. https://doi.org/10.1007/978-981-10-3473-2_23

Kumar R, Ghatak A, Balodi R, Bhagat AP (2018) Decay mechanism of postharvest pathogens and their management using non-chemical and biological approaches. J Postharvest Technol 06:1–11

Li Q, Wu L, Hao J, Luo L, Cao Y, Li J (2015) Biofumigation on postharvest diseases of fruits using a new volatile-producing fungus of *Ceratocystis fimbriata*. PLoS ONE 10:e0132009. https://doi.org/10.1371/journal.pone.0132009

Liu F, Zhan RL, He YB, Zhao YL, Yang SJ, Chang JM (2011) Mechanism of biological control to anthracnoses in mango by antimicrobial Cinnamaldehyde. J Fruit Sci 28(4):651–656

Liu ZQ, Wu ML, Ke ZJ, Liu WB, Li XY (2018) Functional analysis of a regulator of G-protein signaling CgRGS1 in the rubber tree anthracnose fungus *Colletotrichum gloeosporioides*. Arch Microbiol 200(3):391–400. https://doi.org/10.1007/s00203-017-1455-1

Mohammadipour M, Mousivand M, Jouzani GS, Abbasalizadeh S (2009) Molecular and biochemical characterization of Iranian surfactin-producing *Bacillus subtilis* isolates and evaluation of their biocontrol potential against *Aspergillus flavus* and *Colletotrichum gloeosporioides*. Can J Microbiol 55:395–404. https://doi.org/10.1139/W08-141

Pal KK, Gardener BM (2006) Biological control of plant pathogens. Plant Health Instructor Biol Control 7:1–25. https://doi.org/10.1094/PHI-A-2006-1117-02

Pernezny K, Glade B, Marlatt RB (2000) Diseases of avocado in Florida. Plant Pathology Fact Sheet. https://plantpath.ifas.ufl.edu/misc/media/factsheets/pp0021.pdf. Accesed 19 May 2019

Rojo-Báez I, Álvarez-Rodríguez B, García-Estrada RS, León-Félix J, Sañudo-Barajas A, Allende-Molar R (2017) Situación actual de *Colletotrichum* spp. en México: taxonomía, caracterización, patogénesis y control. Rev Mex Fitopatol Mex J Phytopathol 35:549–570. https://doi.org/10.18781/r.mex.fit.1703-9

Sharma RR, Singh D, Singh R (2009) Biological control of postharvest diseases of fruits and vegetables by microbial antagonists. Rev Control Biol. https://doi.org/10.1016/j.biocontrol.2009.05.001

Sharma V, Salwan R, Sharma PN, Kanwar SS (2017) Elucidation of biocontrol mechanisms of *Trichoderma harzianum* against different plant fungal pathogens: universal yet host specific response. Int J Biol Macromol 95:72–79. https://doi.org/10.1016/j.ijbiomac.2016.11.042

SIAP (2019) Boletín mensual de producción de Aguacate, SADER. https://www.gob.mx/cms/uploads/attachment/file/504481/Bolet_n_avance_de_producci_n_de_Aguacate_septiembre_2019.pdf. Accessed 1 Sept 2019

Siddiquee S, Cheong BE, Taslima K, Kausar H, Hasan MM (2012) Separation and identification of volatile compounds from liquid cultures of *Trichoderma harzianum* by GC-MS using three different capillary columns. J Chromatogr Sci 50:358–367. https://doi.org/10.1093/chromsci/bms012

Singh N, Pandey P, Dubey RC, Maheshwari DK (2008) Biological control of root rot fungus Macrophomina phaseolina and growth enhancement of *Pinus roxburghii* (Sarg.) by rhizosphere competent *Bacillus subtilis* BN1. World J Microbiol Biotechnol 24(9):1669. https://doi.org/10.1007/s11274-008-9680-z

Singh RK, Kukrety A, Sharma OP, Poddar MK, Atray N, Ray SS (2017) Synthesis of a novel efficient antioxidant for use in lubes and biodiesel. Pet Chem 57:100–105. https://doi.org/10.1134/S096554411701011X

Trinidad-Ángel E, Ascencio-Valle FDJ, Ulloa OA, Ramírez-Ramíre OC, Ragazzo-Sánchez JA, Calderón-Santoyo M, Bautista Rosales PU (2017) Identificación y caracterización de *Colletotrichum* spp. causante de antracnosis en aguacate de Nayarit, México. Rev Mex Ciencias Agrícolas. https://doi.org/10.29312/remexca.v0i19.664

Wang X, Xu X, Liang Y, Wang Y, Tian C (2018) A Cdc42 homolog in *Colletotrichum gloeosporioides* regulates morphological development and is required for ROS-mediated plant infection. Curr Genet 64(5):1153–1169. https://doi.org/10.1007/s00294-018-0833-9

Wei Y, Pu J, Zhang H, Liu Y, Zhou F, Zhang K, Liu X (2017) The laccase gene (LAC1) is essential for *Colletotrichum gloeosporioides* development and virulence on mango leaves and fruits. Physiol Mol Plant Pathol 99:55–64. https://doi.org/10.1016/j.pmpp.2017.03.005

Wightwick A, Walters R, Allinson G, Reichman S, Menzies N (2010) Environmental risks of fungicides used in horticultural production systems. In: Odise C (ed) Fungicides, 1st edn. InTech, Rijeka, pp 273–304. https://doi.org/10.5772/13032

Willingham SL, Pegg KG, Coates LM, Cooke AW, Dean JR, Langdon PWB, Beasley DR (2001) Field management of avocado postharvest diseases. In: Ben-Arie R, Philosoph-Hadas S (eds) Acta horticulturae, 1st edn. International Society for Horticultural Science (ISHS), Leuven, pp 435–438

Yang HH, Yang SL, Peng KC, Lo CT, Liu SY (2009) Induced proteome of *Trichoderma harzianum* by *Botrytis cinerea*. Mycol Res 113(9):924–932. https://doi.org/10.1016/j.mycres.2009.04.004

Yuan J, Zhao M, Li R, Huang Q, Raza W, Rensing C, Shen Q (2017) Microbial volatile compounds alter the soil microbial community. Environ Sci Pollut Res 24:22485–22493. https://doi.org/10.1007/s11356-017-9839-y

Živković S, Stojanović S, Ivanović Ž, Gavrilović V, Popović T, Balaž J (2010) Screening of antagonistic activity of microorganisms against *Colletotrichum acutatum* and *Colletotrichum gloeosporioides*. Arch Biol Sci 62(3):611–623. https://doi.org/10.2298/ABS1003611Z

Zentmyer GA (1984) Avocado diseases trop. Pest Manag 30:388–400. https://doi.org/10.1080/09670878409370915